Available online at www.sciencedirect.com
SCIENCE DIRECT®
Journal of Sound and Vibration 292 (2006) 390–401
JOURNAL OF SOUND AND VIBRATION
www.elsevier.com/locate/jsvi

Regulating the vibratory motion of beams using shape optimization

J.T. Katsikadelis*, G.C. Tsiatas

School of Civil Engineering, National Technical University of Athens, Zografou Campus, GR-15780 Athens, Greece

Received 27 October 2004; received in revised form 19 July 2005; accepted 2 August 2005
Available online 20 October 2005

Abstract

In this paper, shape optimization is used to regulate the vibrations of an Euler–Bernoulli beam having constant material volume. This is achieved by varying appropriately the beam cross-section and thus its stiffness and mass properties along its length, so that the beam vibrates with its minimum, maximum or a prescribed eigenfrequency as well as with the minimum or maximum difference between two successive eigenfrequencies. The problem is reduced to a nonlinear optimization problem under equality and inequality constraints as well as specified lower and upper bounds. The evaluation of the objective function requires the solution of the free vibration problem of a beam with variable mass and stiffness properties. This problem is solved using the analog equation method (AEM) for hyperbolic differential equations with variable coefficients. Besides its accuracy, this method overcomes the shortcoming of a FEM solution, which would require resizing of the elements and re-computation of their stiffness and mass properties during the optimization process. Certain example problems are presented, which illustrate the method and demonstrate its efficiency.
© 2005 Elsevier Ltd. All rights reserved.

1. Introduction

Shape optimization is a subject which has attracted the interest of the researches for many years. It refers to the optimal design of the shape of structural components and is of great importance in structural and mechanical engineering. The problem consists in finding the best shape of a structural component under certain loading, in order to have minimum weight, or uniformly distributed equivalent stresses or even to control the deflections of the structural components. A shape optimization procedure is an iterative process in which repeated improvements are carried out over successive designs until the optimal design is acceptable. There is an extensive literature on the subject, especially, in the area of structural dynamics [1] on various mathematical and computational techniques which can be applied, including finite element model updating [2] and the use Volterra series [3].

In this paper, we consider the problem of determining the optimum shape of an Euler–Bernoulli beam with a given material volume to regulate its vibratory motion. Namely, we look for the variation law of the cross-section along the beam length so that the beam vibrates with the minimum, the maximum or a prescribed

*Corresponding author. Tel.: +30 2107721654; fax: +30 2107721655.
E-mail addresses: jkats@central.ntua.gr (J.T. Katsikadelis), gtsiatas@central.ntua.gr (G.C. Tsiatas).

0022-460X/$ - see front matter © 2005 Elsevier Ltd. All rights reserved.
doi:10.1016/j.jsv.2005.08.002

eigenfrequency. The problem of minimization or maximization of the difference between two successive eigenfrequencies is also encountered. From both the mathematical and the engineering point of view, it is a very difficult problem. There is an extended literature on the subject which is however limited only to maximization of the fundamental eigenfrequency [4]. The available analytical [4,5] or numerical solutions [6,7], are restricted only to beams with similar cross-sections, namely constrained by the relation $I(x) = aA(x)^n \ (n = 1, 2, 3)$, with $A(x)$ being the area of the cross-section, $I(x)$ its moment of inertia and a a specified constant. All these solutions ignore any restrictions that should be imposed on the rate of change of the cross-section as well as lower bounds resulting from serviceability reasons. It is noteworthy that some optimum solutions lead to zero values of the area A for certain cross-sections as well as to cross-sectional variations for which the beam theory is not valid. These results are unrealistic and, therefore, cannot be used for design. An attempt to get realistic results with FEM is by considering piecewise linear variation in height [8].

In this investigation, the vibratory motion of an Euler–Bernoulli beam with constant volume of the material is regulated by distributing appropriately its mass and stiffness properties along the length. Hence, we seek the variation of the beam cross-section so that the beam vibrates with its minimum, maximum or a prescribed eigenfrequency as well as with the minimum or maximum difference between two successive eigenfrequencies. This problem is reduced to a nonlinear optimization problem under equality and inequality constraints as well as specified lower and upper bounds. The equality constraint results from the condition that the volume of the material is kept constant, while the upper and lower bounds result from the condition that the rate of change of the beam cross-section ensures the validity of the Euler–Bernoulli beam theory for beams with variable cross-section. Finally, the inequality constraint results from serviceability requirements, e.g. the cross-section of the beam should not be less than a certain value. The optimization problem is solved using the successive quadratic programming algorithm and a finite difference gradient. The evaluation of the objective function requires the solution of the free vibration problem of a beam with variable mass and stiffness properties accepting as design variables a set of nodal values, which accurately define the shape of the beam and its rate of variation. This is achieved, thanks to an efficient method for vibration analysis of beams with variable properties. The method is based on the concept of the analog equation [9] as it was developed for beams with variable properties [10]. According to this method, the hyperbolic differential equation with variable coefficients is replaced by an equivalent one pertaining to the transverse deformation of a substitute beam with unit bending stiffness subjected to a quasi-static fictitious load distribution under the same boundary conditions. This method overcomes the drawback of FEM solutions which requires resizing of the beam elements and re-evaluation of their stiffness and mass properties during the iteration process [8]. Several example problems are presented, which illustrate the merits of the method as well as its applicability and efficiency. Moreover, interesting conclusions are drawn regarding the optimum vibrating shapes of the beams.

2. Statement of the problem

2.1. The shape optimization problem for the beam

We consider an Euler–Bernoulli beam with variable cross-section $A = A(x)$ and material density $\bar{\rho}$. The beam is subjected to prescribed boundary conditions. Our problem is to establish the cross-sectional variation so that the beam vibrates with the minimum, the maximum, a prescribed eigenfrequency or with the minimum, maximum difference between two successive eigenfrequencies, while the volume of the material of the beam V_{pr} remains constant. Without restricting the generality the problem of minimization, maximization of the difference between the first two eigenfrequencies is considered. The resulting beam should have no abrupt change of the cross-section so that the Euler beam theory is valid. This requirement imposes the condition that the rate of change of the variation of the cross-section area $h(x)$ is not greater than a certain prescribed value, that is

$$\mathrm{d}h/\mathrm{d}x \simeq \Delta h/\Delta x \leqslant \eta. \tag{1}$$

In order to stay away from these inequality constraints, it is convenient to take as design variables the cross-section h_0 at the end $x = 0$ and the $N + 1$ differences of the adjacent cross-sections $\Delta h_k = h_k - h_{k-1} (k = 1, 2, \ldots, N + 1)$ Δx apart. Thus, the vector of the $N + 2$ design variables is $\mathbf{h} = \{h_0, \Delta h_1, \Delta h_2, \ldots, \Delta h_{N+1}\}^{\mathrm{T}}$ and

the cross-section at the i nodal point is expressed as

$$h_i = h_0 + \sum_{k=1}^{i} \Delta h_k, \quad i = 1, 2, \ldots, N+1. \tag{2}$$

Using the trapezoidal rule to evaluate the volume of the beam, the equality constraint is written as

$$\Delta x \left(\frac{1}{4} h_0 + \frac{3}{4} h_1 + \sum_{i=2}^{N-1} h_i + \frac{3}{4} h_N + \frac{1}{4} h_{N+1} \right) - V_{\text{pr}} = 0. \tag{3}$$

Finally, the inequality constraint from the serviceability may be written as

$$\min h_i \geqslant \varepsilon, \quad i = 0, 1, 2, \ldots, N+1. \tag{4}$$

According to the scope of this paper, the objective function for the beam is

$$\text{minimize } \omega_1(\mathbf{h}), \tag{5a}$$

$$\text{maximize } \omega_1(\mathbf{h}), \tag{5b}$$

$$\text{minimize } \left[1 - \omega_1(\mathbf{h})/\omega_1^{\text{pr}}\right]^2, \tag{5c}$$

$$\text{minimize } [\omega_2(\mathbf{h}) - \omega_1(\mathbf{h})], \tag{5d}$$

$$\text{maximize } [\omega_2(\mathbf{h}) - \omega_1(\mathbf{h})]. \tag{5e}$$

to vibrate with its minimum, maximum, a prescribed fundamental eigenfrequency ω_1^{pr} or with the minimum, maximum difference between the first two eigenfrequencies, respectively. It is apparent that $\omega_1^{\min}$ and $\omega_1^{\max}$ should be first established before specifying ω_1^{pr}.

2.2. The vibration problem for the beam with variable cross-section

The evaluation of the objective function requires the solution of the vibration problem of a beam with variable stiffness and mass properties. This problem is stated as follows.

We consider an initially straight beam of length l having variable bending stiffness $D = D(x) = EI(x)$, which results from variable cross-section. The x-axis coincides with the neutral axis of the beam, which is bent in its plane of symmetry xz under the action of the distributed load $p = p(x, t)$ in the z-direction. We assume that there is no abrupt variation in cross-section of the beam so that the expression for bending moment derived for beams of constant cross-section applies with sufficient accuracy to this case also. Hence, if $w = w(x, t)$ is the transverse deflection of the beam the bending moment and the shear force are given as

$$M = -Dw_{,xx}, \tag{6a}$$

$$Q = M_{,x} = -D_{,x}w_{,xx} - Dw_{,xxx} \tag{6b}$$

and the equation of motion is written as

$$\rho \ddot{w} + L(w) = p(x, t), \tag{7}$$

where

$$L(w) = Dw_{,xxxx} + 2D_{,x}w_{,xxx} + D_{,xx}w_{,xx} \tag{8}$$

with $\rho = \rho(x) = \bar{\rho}A(x)$ being the mass density per unit length of the beam. The beam is subjected to the boundary conditions, which may be written as

$$\beta_1 w(0, t) + \beta_2 Q(0, t) = \beta_3 \quad \text{and} \quad \bar{\beta}_1 w(l, t) + \bar{\beta}_2 Q(l, t) = \bar{\beta}_3, \tag{9a,b}$$

$$\gamma_1 w_{,x}(0, t) + \gamma_2 M(0, t) = \gamma_3 \quad \text{and} \quad \bar{\gamma}_1 w_{,x}(l, t) + \bar{\gamma}_2 M(l, t) = \bar{\gamma}_3 \tag{10a,b}$$

and also to the initial conditions

$$w(x,0)=\tilde{w}(x), \qquad \dot{w}(x,0)=\dot{\tilde{w}}(x), \tag{11a,b}$$

where $\beta_k, \bar{\beta}_k, \gamma_k, \bar{\gamma}_k \quad (k=1,2,3)$ are given constants and $\tilde{w}(x)$, $\dot{\tilde{w}}(x)$ are prescribed functions. Eqs. (9) and (10) describe the most general boundary conditions associated with the problem and can include elastic support or restrain. For example, at an elastically restrained end, say at $x=0$, the boundary condition (9a) becomes, $kw(0,t)+Q(0,t)=P$, that is, $\beta_1=k$, $\beta_2=1$ and $\beta_3=P$; k is the stiffness of the spring and P the external applied force in the z-direction.

3. The AEM solution for the vibration problem

Eq. (7) is solved using the analog equation method (AEM), which for the problem at hand is applied as follows: let $w=w(x,t)$ be the sought solution of Eq. (7), which is four times differentiable in $(0,l)$. Differentiation of w yields

$$w_{,xxxx}=b(x,t). \tag{12}$$

Eq. (12) describes the response of a beam with constant unit stiffness subjected to the fictitious time dependent load $b(x,t)$. It indicates that the solution of Eq. (7) can be established by solving Eq. (12) under the conditions (9)–(10) and (11), provided that the fictitious load distribution b is first determined. Note that Eq. (12) is quasi-static, that is the time considered as a parameter. Eq. (12) is referred to as the analog equation to Eq. (7). The fictitious load is established by developing a procedure based on the boundary integral equation method for one-dimensional problems [10]. Thus, the integral representation of the solution of Eq. (12) is written as

$$w(x,t)=c_1x^3+c_2x^2+c_3x+c_4+\int_0^l G(x,\xi)b(\xi,t)\,\mathrm{d}\xi, \tag{13}$$

where $c_i=c_i(t) \quad (i=1,2,\ldots,4)$ are integration constants to be determined from the boundary conditions and $G(x,\xi)$ is the fundamental solution of Eq. (12) (free space Green's function), that is a particular singular solution of the equation

$$G_{,xxxx}=\delta(x-\xi) \tag{14}$$

with $\delta(x-\xi)$ being the Dirac function. Integrating Eq. (14) yields

$$G=\tfrac{1}{12}|x-\xi|(x-\xi)^2. \tag{15}$$

The derivatives of w are obtained by direct differentiation of Eq. (13). This yields

$$w_{,x}(x,t)=3c_1x^2+2c_2x+c_3+\int_0^l G_{,x}(x,\xi)b(\xi,t)\,\mathrm{d}\xi, \tag{16a}$$

$$w_{,xx}(x,t)=6c_1x+2c_2+\int_0^l G_{,xx}(x,\xi)b(\xi,t)\,\mathrm{d}\xi, \tag{16b}$$

$$w_{,xxx}(x,t)=6c_1+\int_0^l G_{,xxx}(x,\xi)b(\xi,t)\,\mathrm{d}\xi, \tag{16c}$$

$$w_{,xxxx}(x,t)=b(x,t). \tag{16d}$$

In the conventional BEM, the load distribution $b(x,t)$ is known and Eqs. (13), (16) are combined with the boundary conditions (9)–(10) to yield the unknown arbitrary constants $c_i(i=1,2,\ldots,4)$. This, however, cannot be done here since $b(x,t)$ is unknown. For this purpose, an additional integral equation is derived, which permits the establishment of $b(x,t)$. This equation results by applying the operator $\rho(\mathrm{d}^2/\mathrm{d}t^2)+L$ to

Eq. (13). This yields

$$\rho\left[\ddot{c}_1x^3+\ddot{c}_2x^2+\ddot{c}_3x+\ddot{c}_4+\int_0^l G(x,\xi)\ddot{b}(\xi,t)\,\mathrm{d}\xi\right]$$
$$+c_1L\left(x^3\right)+c_2L\left(x^2\right)+c_3L(x)+c_4L(1)+\int_0^l L(G(x,\xi))b(\xi,t)\,\mathrm{d}\xi=p(x,t). \tag{17}$$

Eq. (17) is a domain integral equation for $b(x,t)$, which can be solved numerically as follows.

The interval $(0,l)$ is divided into N equal elements (see Fig. 1) on which $b(x,t)$ is assumed to vary according to a certain law (constant, linear, parabolic, etc). The constant element assumption is employed here, because the numerical implementation becomes very simple and the obtained numerical results are very good.

After discretization of Eq. (13) we obtain

$$w(x,t)=\sum_{j=1}^{4}x^{4-j}c_j(t)+b(\xi_j)\sum_{j=1}^{N}\int_j G(x,\xi)\,\mathrm{d}\xi \tag{18}$$

or

$$w(x,t)=\mathbf{H}(x)\mathbf{c}+\mathbf{G}(x)\mathbf{b}, \tag{19}$$

where $\mathbf{G}(x)$ is an $1\times N$ known matrix originating from the integration of the kernel $G(x,\xi)$ on the elements; $\mathbf{H}(x)=\begin{bmatrix}x^3 & x^2 & x & 1\end{bmatrix}$; $\mathbf{b}=\{b_1,b_2,\ldots,b_N\}^{\mathrm{T}}$ is the vector containing the values of the fictitious load at the nodal points and $\mathbf{c}=\{c_1,c_2,c_3,c_4\}^{\mathrm{T}}$. Similarly, we obtain for Eqs. (16a)–(16c)

$$w_{,x}(x,t)=\mathbf{H}_x(x)\mathbf{c}+\mathbf{G}_x(x)\mathbf{b}, \tag{20a}$$

$$w_{,xx}(x,t)=\mathbf{H}_{xx}(x)\mathbf{c}+\mathbf{G}_{xx}(x)\mathbf{b}, \tag{20b}$$

$$w_{,xxx}(x,t)=\mathbf{H}_{xxx}(x)\mathbf{c}+\mathbf{G}_{xxx}(x)\mathbf{b}, \tag{20c}$$

$$w_{,xxxx}(x,t)=\mathbf{b}, \tag{20d}$$

where $\mathbf{G}_x(x)$, $\mathbf{G}_{xx}(x)$, $\mathbf{G}_{xxx}(x)$, are $1\times N$ known matrices, originating from the integration of the derivatives of the kernel $G(x,\xi)$ and $\mathbf{H}_x(x)$, $\mathbf{H}_{xx}(x)$, $\mathbf{H}_{xxx}(x)$ are 1×4 known matrices resulting from the differentiation of $\mathbf{H}(x)$.

First, Eqs. (19) and (20) are applied to the end nodal points $x=0$ and $x=l$. This yields

$$w(0,t)=\mathbf{H}(0)\mathbf{c}+\mathbf{G}(0)\mathbf{b}, \qquad w(l,t)=\mathbf{H}(l)\mathbf{c}+\mathbf{G}(l)\mathbf{b}, \tag{21a}$$

$$w_{,x}(0,t)=\mathbf{H}_x(0)\mathbf{c}+\mathbf{G}_x(0)\mathbf{b}, \qquad w_{,x}(l,t)=\mathbf{H}_x(l)\mathbf{c}+\mathbf{G}_x(l)\mathbf{b}, \tag{21b}$$

$$w_{,xx}(0,t)=\mathbf{H}_{xx}(0)\mathbf{c}+\mathbf{G}_{xx}(0)\mathbf{b}, \qquad w_{,xx}(l,t)=\mathbf{H}_{xx}(l)\mathbf{c}+\mathbf{G}_{xx}(l)\mathbf{b}, \tag{21c}$$

$$w_{,xxx}(0,t)=\mathbf{H}_{xxx}(0)\mathbf{c}+\mathbf{G}_{xxx}(0)\mathbf{b}, \qquad w_{,xxx}(l,t)=\mathbf{H}_{xxx}(l)\mathbf{c}+\mathbf{G}_{xxx}(l)\mathbf{b}. \tag{21d}$$

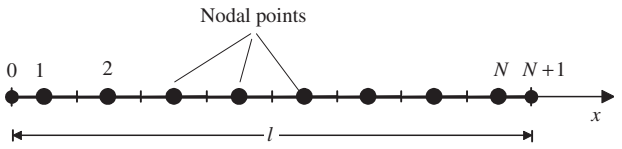

Fig. 1. Descretization of the interval and distribution of the nodal points.

Substituting Eqs. (21) into the boundary conditions (9)–(10) gives

$$\begin{bmatrix} \beta_1\mathbf{H}(0)-\beta_2 D_{,x}(0)\mathbf{H}_{xx}(0)-\beta_2 D(0)\mathbf{H}_{xxx}(0) \\ \bar{\beta}_1\mathbf{H}(l)-\bar{\beta}_2 D_{,x}(l)\mathbf{H}_{xx}(l)-\bar{\beta}_2 D_{,x}(l)\mathbf{H}_{xxx}(l) \\ \gamma_1\mathbf{H}_x(0)-\gamma_2 D(0)\mathbf{H}_{xx}(0) \\ \bar{\gamma}_1\mathbf{H}_x(l)-\bar{\gamma}_2 D(l)\mathbf{H}_{xx}(l) \end{bmatrix}\mathbf{c}+\begin{bmatrix} \beta_1\mathbf{G}(0)-\beta_2 D_{,x}(0)\mathbf{G}_{xx}(0)-\beta_2 D(0)\mathbf{G}_{xxx}(0) \\ \bar{\beta}_1\mathbf{G}(l)-\bar{\beta}_2 D_{,x}(l)\mathbf{G}_{xx}(l)-\bar{\beta}_2 D_{,x}(l)\mathbf{G}_{xxx}(l) \\ \gamma_1\mathbf{G}_x(0)-\gamma_2 D(0)\mathbf{G}_{xx}(0) \\ \bar{\gamma}_1\mathbf{G}_x(l)-\bar{\gamma}_2 D(l)\mathbf{G}_{xx}(l) \end{bmatrix}\mathbf{b}=\begin{bmatrix} \beta_3 \\ \bar{\beta}_3 \\ \gamma_3 \\ \bar{\gamma}_3 \end{bmatrix}. \tag{22}$$

Solving Eq. (22) for $\mathbf{c}$ yields

$$\mathbf{c}=\mathbf{E}\mathbf{b}+\mathbf{e} \tag{23}$$

in which $\mathbf{E}$ is a known $4\times N$ rectangular matrix and $\mathbf{e}$ is a known 4×1 vector.

Subsequently, applying Eq. (17) to the N interior nodal points yields

$$\boldsymbol{\rho}\mathbf{H}\ddot{\mathbf{c}}+\boldsymbol{\rho}\mathbf{G}\ddot{\mathbf{b}}+\mathbf{S}\mathbf{c}+\mathbf{R}\mathbf{b}=\mathbf{p}. \tag{24}$$

The matrices $\mathbf{S}$ and $\mathbf{R}$ are evaluated from the expressions

$$\mathbf{R}=\mathbf{D}+2\mathbf{D}_x\mathbf{G}_{xxx}+\mathbf{D}_{xx}\mathbf{G}_{xx}, \tag{25}$$

$$\mathbf{S}=\mathbf{H}_{xx}\mathbf{D}_{xx}+2\mathbf{H}_{xxx}\mathbf{D}_x, \tag{26}$$

where $\mathbf{G}=\mathbf{G}(x_i)$, $\mathbf{G}_{xx}=\mathbf{G}_{xx}(x_i)$, $\mathbf{G}_{xxx}=\mathbf{G}_{xxx}(x_i)$, $i=1,2,\ldots,N$, are $N\times N$ known matrices originating from the integration of the kernel function, and its derivatives on the elements; $\mathbf{H}=\mathbf{H}(x_i)$, $\mathbf{H}_x=\mathbf{H}_x(x_i)$, $\mathbf{H}_{xxx}=\mathbf{H}_{xxx}(x_i)$, $i=1,2,\ldots,N$, are also $N\times 4$ known matrices; $\mathbf{D},\mathbf{D}_x,\mathbf{D}_{xx}$ are $N\times N$ known diagonal matrices including the values of the stiffness and its derivatives at the nodal points and $\mathbf{p}$ is the vector containing the values of the external distributed load at the nodal points.

Eq. (23) is used to eliminate $\mathbf{c}$ from Eq. (24). This yields

$$\mathbf{M}\ddot{\mathbf{b}}+\mathbf{K}\mathbf{b}=\mathbf{F}, \tag{27}$$

which is the semidiscretized equation of motion with

$$\mathbf{M}=\boldsymbol{\rho}(\mathbf{G}+\mathbf{H}\mathbf{E}), \tag{28a}$$

$$\mathbf{K}=\mathbf{D}+\mathbf{D}_{xx}(\mathbf{G}_{xx}+\mathbf{H}_{xx}\mathbf{E})+2\mathbf{D}_x(\mathbf{G}_{xxx}+\mathbf{H}_{xxx}\mathbf{E}), \tag{28b}$$

$$\mathbf{F}=\mathbf{p}-(\mathbf{D}_{xx}\mathbf{H}_{xx}+2\mathbf{D}_x\mathbf{H}_{xxx})\mathbf{e} \tag{28c}$$

playing the role of the generalized mass matrix, stiffness matrix and force vector, respectively. The associated initial conditions result from Eqs. (11a,b). Thus, we have

$$\mathbf{b}(0)=(\mathbf{G}+\mathbf{H}\mathbf{E})^{-1}(\tilde{\mathbf{w}}_0-\mathbf{H}\mathbf{e}),\quad \dot{\mathbf{b}}(0)=(\mathbf{G}+\mathbf{H}\mathbf{E})^{-1}\dot{\tilde{\mathbf{w}}}_0. \tag{29}$$

Eq. (27) can be solved numerically to establish the vector $\mathbf{b}(t)$ and backsubstitution in Eq. (23) gives $\mathbf{c}$. Once $\mathbf{b}(t)$ and $\mathbf{c}$ are known, the deflection and its derivatives are established from Eqs. (19) and (20).

Free vibrations: For free vibrations it is $\mathbf{F}=\mathbf{0}$, and by setting $\mathbf{b}(t)=\mathbf{B}e^{-i\omega t}$ Eq. (27) becomes

$$(-\omega^2\mathbf{M}+\mathbf{K})\mathbf{B}=\mathbf{0}, \tag{30}$$

which is a generalized eigenvalue problem of linear algebra from which the eigenfrequencies ω and eigenvectors $\mathbf{B}$ are established. The eigenvectors may be used in Eq. (19) to establish the mode shapes of the beam.

4. Numerical examples

On the basis of the procedure described in previous section a FORTRAN program has been written for establishing the optimum vibrating shapes. The optimization procedure was carried out using the subroutine DNCONF from the IMSL library. This subroutine uses the successive quadratic programming (SQP) method

and is based on the subroutine NLPQL developed by Schittkowski [11]. The required gradients of the objective functions and constraints are calculated internally using the finite difference method. In all examples, the results have been obtained using $N = 51$ elements.

Example 1. *Beam with a similar circular cross-section*: For the comparison of the results with those available from the literature, the maximization of the fundamental eigenfrequency of a simply supported beam having initially a constant circular cross-section has been studied. The employed data are $l = 1.0\,\mathrm{m}$, initial radius $r = \sqrt{40}\,\mathrm{mm}$ and $I(x) = \pi r(x)^4/4 = A(x)^2/4\pi$. In Table 1 the computed ratio $\omega_1^{\max}/\omega_1$ for various values of the parameter η is shown as compared with those obtained from an analytical [5] and a FEM [6] solution without restriction on the rate of change. As it was anticipated, for large values of η the computed value coincides with the analytical one.

Example 2. *Steel beam with a rectangular cross-section*: The optimum vibrating shapes of a steel beam with length $l = 5.0\,\mathrm{m}$ having initially a constant rectangular cross-section $b \times h$, has been studied. The employed data are: $E = 2.1 \times 10^8\,\mathrm{kN/m^2}$, $b = 0.1\,\mathrm{m}$, $h = 0.30\,\mathrm{m}$ and $\bar{\rho} = 7850\,\mathrm{kg/m^3}$. Three types of boundary conditions are considered (i) fixed–fixed ($\omega_1 = 400.85\,\mathrm{rad/s}$), (ii) simply supported ($\omega_1 = 176.83\,\mathrm{rad/s}$) and (iii) cantilever ($\omega_1 = 63.00\,\mathrm{rad/s}$); ω_1 is the fundamental eigenfrequency of the beam with constant rectangular cross-section. In all three cases the width b and the volume of the beam $V = bhl$ were kept constant. Hence, the design parameters designate the height of the beam at the nodal points. The results obtained for $\eta = 0.1$ and $\varepsilon = 0.1h$ are shown in Figs. 2–4.

Example 3. *Steel beam with an I-section*: The optimum vibrating shapes of a steel **I**-section beam with length $l = 10.0\,\mathrm{m}$, has been studied. The initial cross-section is constant and it is constructed from a pair of identical flange plates $b = 100\,\mathrm{mm}$ wide by $t_f = 15\,\mathrm{mm}$ thick and a web plate $t_w = 15\,\mathrm{mm}$ thick with height $h_w = 500\,\mathrm{mm}$ (see Fig. 5). The other data are: $E = 2.1 \times 10^8\,\mathrm{kN/m^2}$, $\bar{\rho} = 7850\,\mathrm{kg/m^3}$. Three types of boundary conditions are considered (i) fixed–fixed ($\omega_1 = 212.87\,\mathrm{rad/s}$, $\omega_2 = 586.93\,\mathrm{rad/s}$), (ii) simply supported ($\omega_1 = 93.90\,\mathrm{rad/s}$, $\omega_2 = 375.69\,\mathrm{rad/s}$) and (iii) cantilever ($\omega_1 = 33.45\,\mathrm{rad/s}$, $\omega_2 = 209.71\,\mathrm{rad/s}$); ω_1, ω_2 are the first two eigenfrequencies of the constant section. In all three cases the volume of the material, i.e. $V = (t_w h_w + 2t_f b)l$, was kept constant. For a realistic construction of the optimum beam only the web height h_w was allowed to vary. Thus, the design parameters are the height of the beam at the nodal points. The obtained results for $\varepsilon = 0.1h_w$ are shown in Figs. 6–14. More specifically, in Figs. 6–8 the dependence of the ratios

Table 1
Example 1: The ratio $\omega_1^{\max}/\omega_1$ for various values of η

Proposed				[5]	[6]
$\eta = 0.20$	$\eta = 0.30$	$\eta = 0.40$	$\eta = 0.50$	No constraint on η	
1.049	1.058	1.063	1.066	1.066	1.060

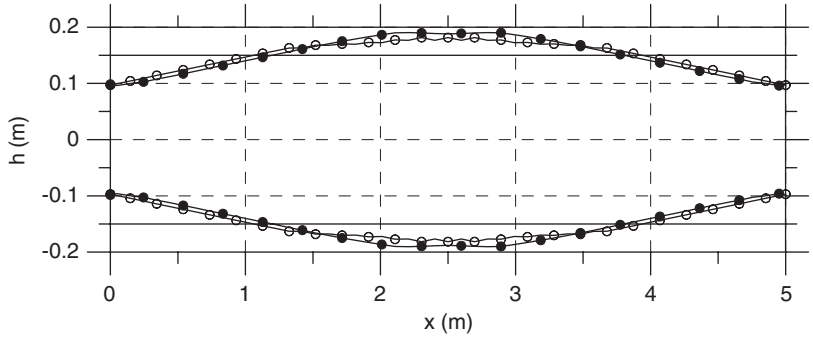

Fig. 2. Example 2: Optimal height profiles of the fixed–fixed beam. —— ω_1, —○— $\omega_1^{\min} = 1.46\%\omega_1$, —●— $\omega_1^{\mathrm{pr}} = 80.00\%\omega_1$.

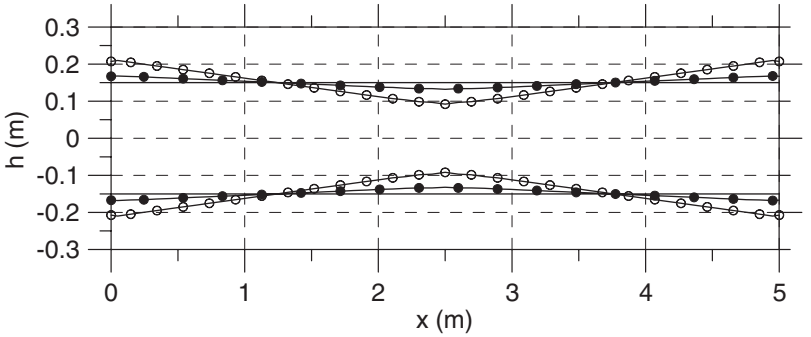

Fig. 3. Example 2: Optimal height profiles of the simply supported beam. —— ω_1, —○— $\omega_1^{\min} = 3.20\%\omega_1$, —●— $\omega_1^{\text{pr}} = 90.00\%\omega_1$.

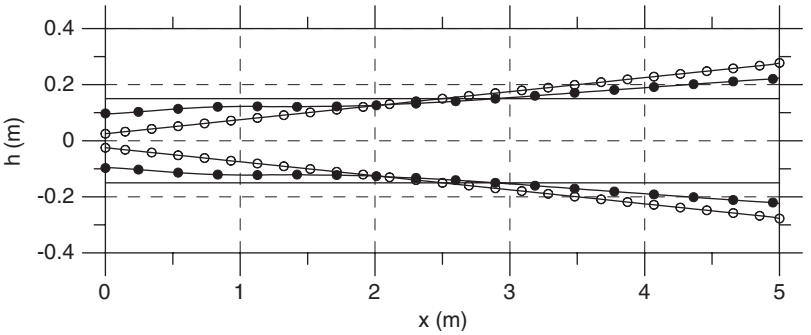

Fig. 4. Example 2: Optimal height profiles of the cantilever beam. —— ω_1, —○— $\omega_1^{\min} = 13.18\%\omega_1$, —●— $\omega_1^{\text{pr}} = 60.00\%\omega_1$.

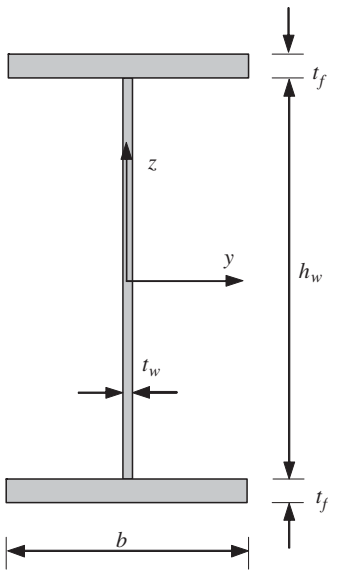

Fig. 5. Example 3: Cross-section of the Steel I-section beam.

$\omega_1^{\min}/\omega_1$ and $\omega_1^{\max}/\omega_1$ on the height rate of change η is presented, while in Figs. 9–11 the profiles of the upper half of the height variation along the beam axis for various values of η are shown. Moreover, the profiles of the upper half of the height variation along the beam axis are shown in Figs. 12–14 for the minimum, maximum difference of the first two eigenfrequencies.

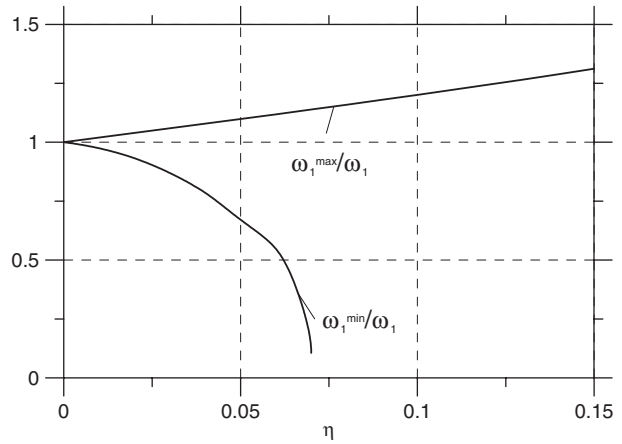

Fig. 6. Example 3: Dependence of the ratios $\omega_1^{\min}/\omega_1$ and $\omega_1^{\max}/\omega_1$ on the height rate of change η for the fixed–fixed beam.

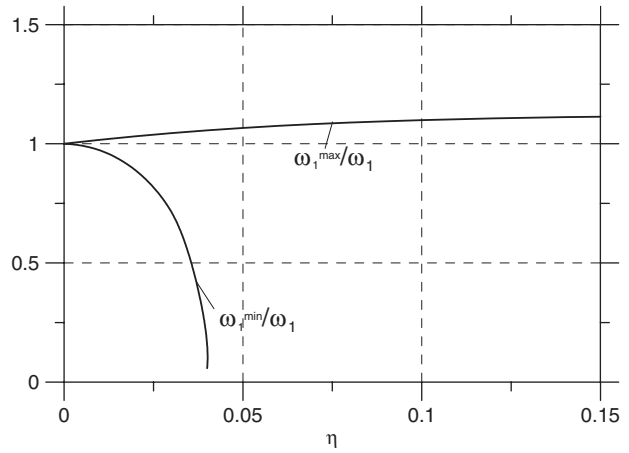

Fig. 7. Example 3: Dependence of the ratios $\omega_1^{\min}/\omega_1$ and $\omega_1^{\max}/\omega_1$ on the height rate of change η for the simply supported beam.

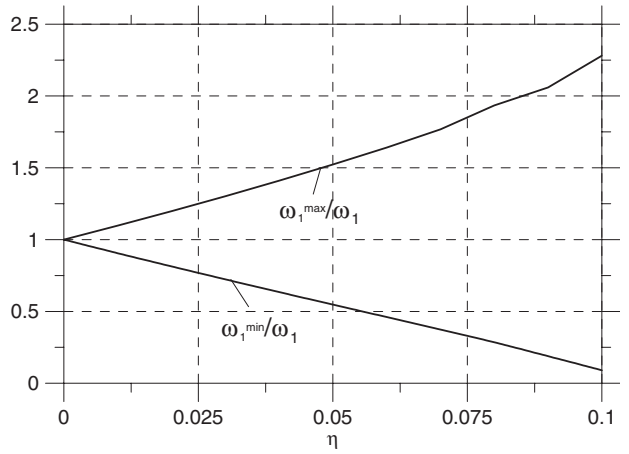

Fig. 8. Example 3: Dependence of the ratios $\omega_1^{\min}/\omega_1$ and $\omega_1^{\max}/\omega_1$ on the height rate of change η for the cantilever beam.

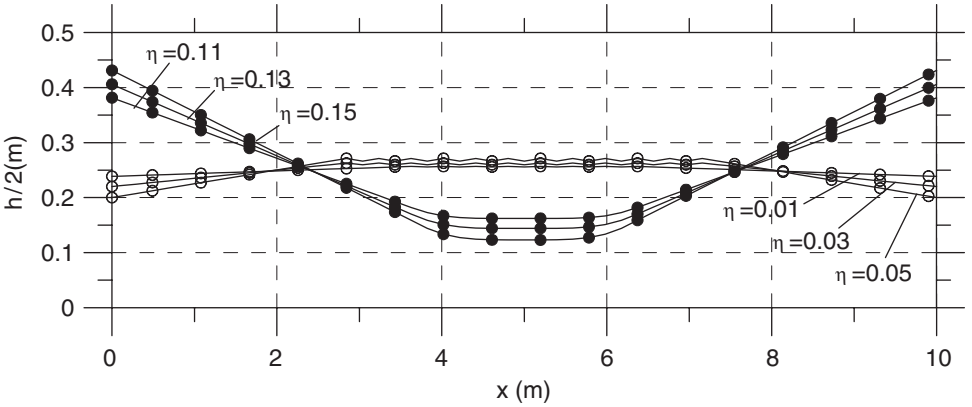

Fig. 9. Example 3: Profiles of the upper half of the height for various values of η for the fixed–fixed beam. —○— $\omega_1^{\min}$, —●— $\omega_1^{\max}$.

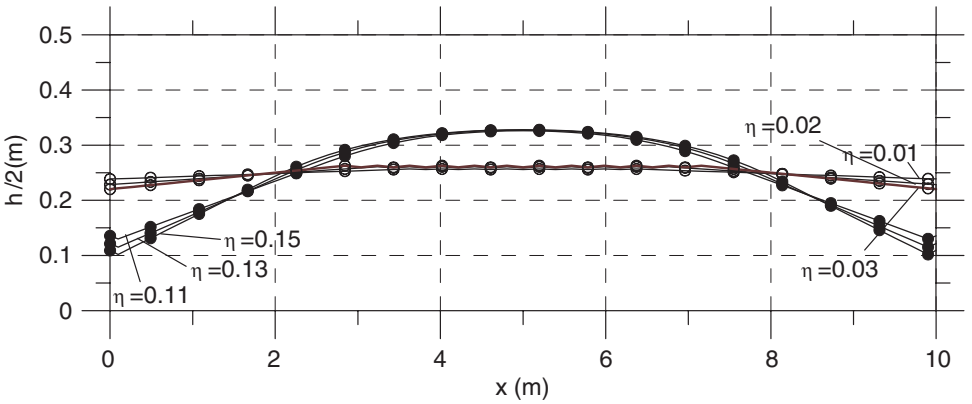

Fig. 10. Example 3: Profiles of the upper half of the height for various values of η for the simply supported beam. —○— $\omega_1^{\min}$, —●— $\omega_1^{\max}$.

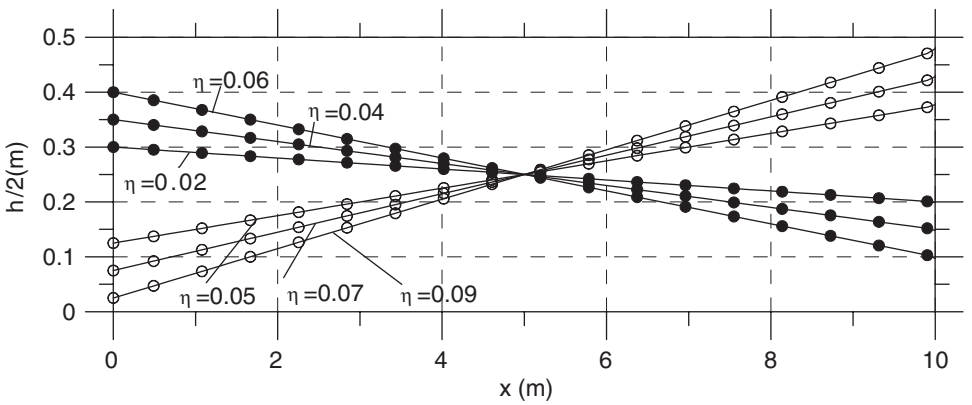

Fig. 11. Example 3: Profiles of the upper half of the height for various values of η for the cantilever beam. —○— $\omega_1^{\min}$, —●— $\omega_1^{\max}$.

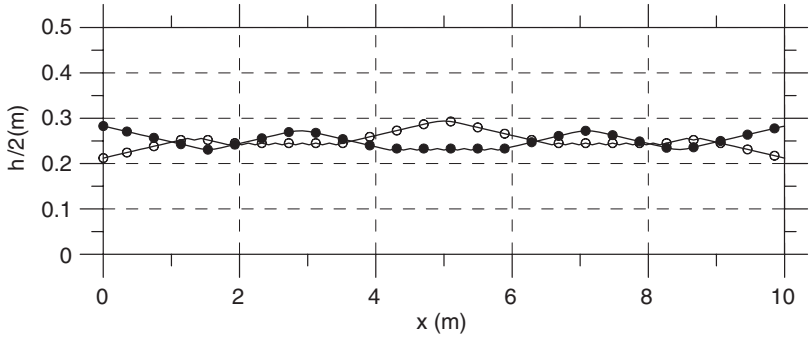

Fig. 12. Example 3: Profiles of the upper half of the height for the fixed–fixed beam. Height rate of change $\eta = 0.07$. —○— $(\omega_2 - \omega_1)^{\min} = 77.70\%(\omega_2 - \omega_1)$, —●— $(\omega_2 - \omega_1)^{\max} = 120.23\%(\omega_2 - \omega_1)$.

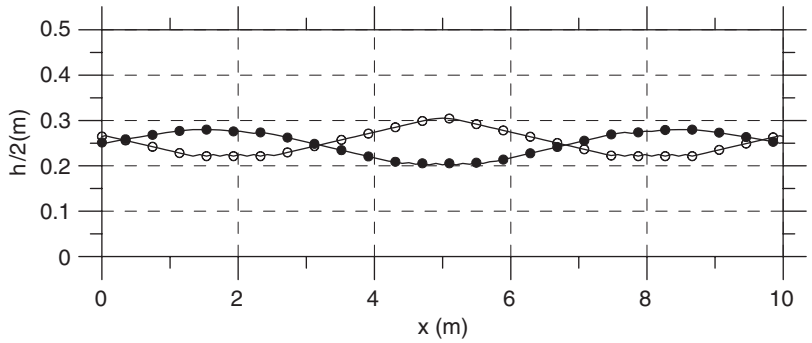

Fig. 13. Example 3: Profiles of the upper half of the height for the simply supported beam. Height rate of change $\eta = 0.07$. —○— $(\omega_2 - \omega_1)^{\min} = 78.90\%(\omega_2 - \omega_1)$, —●— $(\omega_2 - \omega_1)^{\max} = 130.10\%(\omega_2 - \omega_1)$.

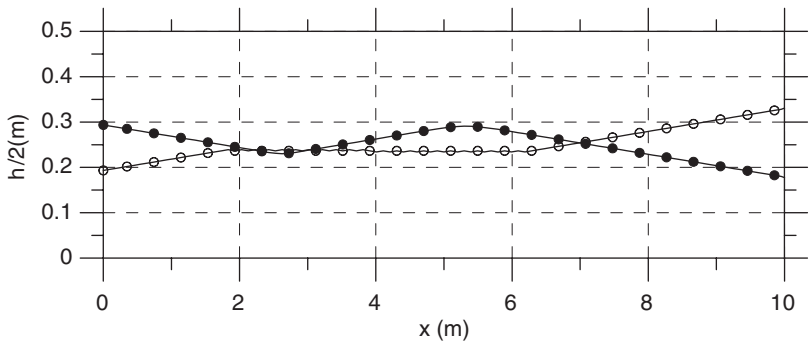

Fig. 14. Example 3: Profiles of the upper half of the height for the cantilever beam. Height rate of change $\eta = 0.05$. —○— $(\omega_2 - \omega_1)^{\min} = 37.96\%(\omega_2 - \omega_1)$, —●— $(\omega_2 - \omega_1)^{\max} = 111.49\%(\omega_2 - \omega_1)$.

5. Conclusions

In this paper, the optimum vibrating shapes of an Euler–Bernoulli beam with constant volume of the material are studied. This problem is reduced to a nonlinear optimization problem under equality and inequality constraints as well as specified lower and upper bounds. From the presented analysis and the numerical examples the following main conclusions can be drawn.

(a) An integrated solution procedure is presented for regulating the vibration of beams using shape optimization.

(b) The method is free of cross-sectional similarity constraints and permits the control of the rate of change of the cross-section so that the Euler–Bernoulli theory is valid (no abrupt change of the cross-section). These inequality constraints are converted to simple lower and upper bounds in order to improve the optimization procedure.
(c) The cross-section satisfies inequality constraints resulting from serviceability requirements for the beam, e.g. the cross-section should not be less than a certain value.
(d) The solution procedure of the free vibration problem of a beam with variable mass and stiffness properties is achieved thanks to AEM. This method provides a direct solution of the differential equation of motion and overcomes the shortcoming of FEM solutions, which require resizing of the elements and re-computation of their stiffness and mass properties during the optimization process.
(e) The ratio $\omega_1^{\max}/\omega_1$ increases monotonically with the height rate of change η. The opposite happens for the ratio $\omega_1^{\min}/\omega_1$.
(f) In obtaining $\omega_1^{\min}$ the material is shifted away from stiff supports, while for $\omega_1^{\max}$ the opposite is true.

References

[1] C. Zang, M.I. Friswell, J.E. Mottershead, A review of robust optimal design and its application in dynamics, *Computers & Structures* 83 (2005) 315–326.
[2] C. Mares, J.E. Mottershead, M.I. Friswell, Results obtained by minimizing natural-frequency errors and using physical reasoning, *Mechanical Systems and Signal Processing* 17 (2003) 39–46.
[3] K. Worden, G. Manson, A Volterra series approximation to the coherence of the Duffing oscillator, *Journal of Sound and Vibration* 286 (2005) 529–547.
[4] R.T. Haftka, Z. Gurdal, M.P. Kamat, *Elements of Structural Optimization*, second ed., Kluwer Academic Publishers, Dordrecht, 1990.
[5] F.I. Niordson, On the optimal design of a vibrating beam, *Quarterly of Applied Mathematics* 23 (1965) 47–53.
[6] M.P. Kamat, G.J. Simitses, Optimal beam frequencies by the finite element displacement method, *International Journal of Solids and Structures* 9 (1973) 415–429.
[7] M.P. Kamat, Effect of shear deformations and rotary inertia on optimum beam frequencies, *International Journal for Numerical Methods in Engineering* 9 (1975) 51–62.
[8] D.P. Thambiratnam, V. Thevendran, Optimum vibrating shapes of beams and circular plates, *Journal of Sound and Vibration* 121 (1988) 13–23.
[9] J.T. Katsikadelis, The analog equation method: a boundary-only integral equation method for nonlinear static and dynamic problems in general bodies,, *Theoretical and Applied Mechanics* 27 (2002) 13–38.
[10] J.T. Katsikadelis, G.C. Tsiatas, Nonlinear dynamic analysis of beams with variable stiffness, *Journal of Sound and Vibration* 270 (2004) 847–863.
[11] K. Schittkowski, NLPQL: a FORTRAN subroutine solving constrained nonlinear programming problems, *Annals of Operations Research* 5 (1986) 485–500.